

Appendix

Transneuronal Dpr12/DIP- δ interactions facilitate compartmentalized dopaminergic innervation of *Drosophila* mushroom body axons

Bavat Bornstein¹, Hagar Meltzer^{1*}, Ruth Adler¹, Idan Alyagor¹, Victoria Berkun¹, Gideon Cummings¹, Fabienne Reh², Hadas Keren-Shaul^{3,4}, Eyal David³, Thomas Riemensperger² and Oren Schuldiner^{1*#}

Correspondence to: oren.schuldiner@weizmann.ac.il
hagar.meltzer@weizmann.ac.il

Table of contents:

| | |
|--|-----|
| List of genotypes | 2-4 |
| Appendix Figure S1: Additional data regarding Dpr12 and DIP- δ protein localization | 5 |
| Appendix Figure S2: MBON- γ 3 innervation of the MB γ -lobe in Dpr12 mutant brains | 6 |
| Appendix Table S1: EM-skeletons used for model generation | 7 |
| Appendix Table S2: List of drivers used in the current study | 8 |

List of genotypes used in this study:

hsFLP is *y,w,hsFLP122*; tdT is *tdTomato*; mtdT-HA is *mtdTomato-3xHA*; 40A and G13 are FRTs on 2L and 2R respectively; R71G10 is *GMR71G10-Gal4*; R18H09 is *GMR18H09-Gal4*; R58E02 is *GMR58E02-Gal4*; R10G03 is *GMR10G03-Gal4*; R48H011 is *GMR48H011-Gal4*; G80 is *TubP-Gal80*. Males and females were used interchangeably but only the female genotype is mentioned.

Figure 1

(C) *y, w; R71G10, UAS-mCD8-GFP/+; R71G10, UAS-Dcr-2/+*
(D) *y, w; R71G10, UAS-mCD8-GFP/+; R71G10, UAS-Dcr-2/ TRiP.JF03210(dpr12-RNAi)*
(E) *y, w; R71G10, UAS-mCD8-GFP/+; UAS-Cas9.C*
(F) *y, w; R71G10, UAS-mCD8-GFP/+; UAS-Cas9.C/dpr12-gRNA*
(G-I) *y, w; UAS-mCD8-GFP/+; R71G10/+*
(J) *y, w; UAS-mCD8-GFP/+; R71G10/UAS-Dpr12*
(K-M) *y, w; 40A, dpr12 Δ^{50-81} , G13/40A, dpr12 Δ^{50-81} , G13; R71G10, UAS-mCD8-GFP/+*
(N) *y, w; 40A, dpr12 Δ^{50-81} , G13/40A, dpr12 Δ^{50-81} , G13; R71G10, UAS-mCD8-GFP/UAS-Dpr12*

Figure 2

(A-C, G-I) *hsFLP, UAS-mCD8-GFP; Gal80, FRT40A/FRT40A; R71G10, UAS-Dcr-2/+*
(D-F, J-L) *hsFLP, UAS-mCD8-GFP; Gal80, FRT40A/FRT40A; R71G10, UAS-Dcr-2/ TRiP.JF03210 (dpr12-RNAi)*
(O) *y, w; UAS-mCD8-GFP/+; R18H09/+*

Figure 3

(A-C) *y, w; Dpr12^{GFSTF}/+*
(D) *y, w; UAS-CD4-tdT/Dpr12^{GFSTF}; R18H09/+*
(E-G) *y, w;; DIP- δ ^{GFSTF}/+*
(H) *y, w; UAS-CD4-tdT/+; DIP- δ ^{GFSTF}/R18H09*

Figure 4

(A-C) *y, w; R71G10-QF2, QUAS-mtdT-HA/+; DIP- δ ^{T2A-Gal4}/+*
(D) *y, w; R71G10-QF2, QUAS-mtdT-HA/UAS-DIP- δ ; DIP- δ ^{T2A-Gal4}/+*
(E-G) *y, w; R71G10-QF2, QUAS-mtdT-HA/+; DIP- δ ^{T2A-Gal4}/DIP- δ ^{T2A-Gal4}*
(H) *y, w; R71G10-QF2, QUAS-mtdT-HA/UAS-DIP- δ ; DIP- δ ^{T2A-Gal4}/DIP- δ ^{T2A-Gal4}*
(J) *y, w; UAS-DIP- δ -RNAi/R71G10-QF2, QUAS-mtdT-HA; Repo-Gal4, UAS-mCD8-GFP/+*
(K) *y, w; UAS-DIP- δ -RNAi/R71G10-QF2, QUAS-mtdT-HA; OK107-Gal4*
(L) *C155-Gal4; UAS-DIP- δ -RNAi/R71G10-QF2, QUAS-mtdT-HA*
(M) *y, w; UAS-DIP- δ -RNAi/R71G10-QF2, QUAS-mtdT-HA; DIP- δ ^{T2A-Gal4}/+*

Figure 5

(A) *UAS-mCD8-RFP; R53C03-p65.AD/+; DIP- δ ^{GFSTF}/R24E12-GAL4.DBD*
(B) *UAS-mCD8-RFP; R53C03-p65.AD/UAS-DTi; DIP- δ ^{GFSTF}/R24E12-GAL4.DBD*

(C) y, w; UAS-CD4-tdT/+; DIP- δ ^{GFSTF}/R58E02
(D) y, w; UAS-CD4-tdT/UAS-DTi; DIP- δ ^{GFSTF}/R58E02
(E-G) hsFLP, UAS-mCD8-GFP; Gal80, FRT40A/FRT40A; *DIP- δ ^{T2A-Gal4}/+*

Figure 6

(A-D) y, w; Dpr12^{GFSTF}/+; *DIP- δ ^{T2A-Gal4}/DIP- δ ^{T2A-Gal4}*
(E-H) y, w; 40A, *dpr12 Δ ⁵⁰⁻⁸¹*, G13/40A, *dpr12 Δ ⁵⁰⁻⁸¹*, G13; DIP- δ ^{GFSTF}/+
(I) y, w; Dpr12^{GFSTF}/+; UAS-DIP- δ -T2A-tdT/+
(J) y, w; Dpr12^{GFSTF} /R30G08-p65.AD; R48B03-GAL4.DBD/ UAS-DIP- δ -T2A-tdT

Figure 7

(A) y, w; 40A, *dpr12 Δ ⁵⁰⁻⁸¹*, G13/+; R10G03/UAS-mCD8-GFP
(B) y, w; 40A, *dpr12 Δ ⁵⁰⁻⁸¹*, G13/40A, *dpr12 Δ ⁵⁰⁻⁸¹*, G13; R10G03/UAS-mCD8-GFP
(C) y, w; 40A, *dpr12 Δ ⁵⁰⁻⁸¹*, G13/+; R48H011/UAS-mCD8-GFP
(D) y, w; 40A, *dpr12 Δ ⁵⁰⁻⁸¹*, G13/40A, *dpr12 Δ ⁵⁰⁻⁸¹*, G13; R48H011/UAS-mCD8-GFP
(E) y, w; 40A, *dpr12 Δ ⁵⁰⁻⁸¹*, G13/+; R18H09/UAS-mCD8-GFP
(F) y, w; 40A, *dpr12 Δ ⁵⁰⁻⁸¹*, G13/40A, *dpr12 Δ ⁵⁰⁻⁸¹*, G13; R18H09/UAS-mCD8-GFP
(G) w¹¹¹⁸
(H) w¹¹¹⁸; 40A, *dpr12 Δ ⁵⁰⁻⁸¹*, G13/40A, *dpr12 Δ ⁵⁰⁻⁸¹*, G13

Figure 8

(A) y, w; R71G10-QF2, QUAS-mtdT-HA/+; *DIP- δ ^{T2A-Gal4}/DIP- δ ¹⁻¹¹⁹*
(B) y, w; R71G10-QF2, QUAS-mtdT-HA/+; *DIP- δ ^{T2A-Gal4}/DIP- δ ¹⁻¹¹⁹*, UAS-DIP- α
(C) y,w; Dpr12^{GFSTF}/+; *DIP- δ ¹⁻¹¹⁹*, UAS-DIP- α /+
(D) y,w; Dpr12^{GFSTF}/+; *DIP- δ ¹⁻¹¹⁹*, UAS-DIP- α /DIP- δ ^{T2A-Gal4}
(E) y, w; 40A, *dpr12 Δ ⁵⁰⁻⁸¹*, G13/40A, *dpr12 Δ ⁵⁰⁻⁸¹*, G13; *DIP- δ ^{T2A-Gal4}*/ UAS-mtdT
(F) y, w; 40A, *dpr12 Δ ⁵⁰⁻⁸¹*, G13/40A, *dpr12 Δ ⁵⁰⁻⁸¹*, G13; *DIP- δ ^{T2A-Gal4}*/ UAS-DIP- α -T2A-tdT

Figure EV1

(A)
y, w; R71G10, UAS-mCD8-GFP/+; R71G10, UAS-Dcr-2/ TRiP.JF03306(Dpr5-RNAi)
y, w; UAS-mCD8-GFP/+; R71G10/ TRiP.JF03172 (Dpr8-RNAi)
y, w; UAS-mCD8-GFP/+; R71G10/ TRiP.HMS00288 (Dpr9-RNAi)
y, w; R71G10, UAS-mCD8-GFP/+; R71G10, UAS-Dcr-2/ TRiP.JF02920 (Dpr10-RNAi)
y, w; R71G10, UAS-mCD8-GFP/+; R71G10, UAS-Dcr-2/ TRiP.JF03210(Dpr12-RNAi)
y, w; UAS-mCD8-GFP/+; R71G10/ TRiP.GL01238 (Dpr17-RNAi)
y, w; R71G10, UAS-mCD8-GFP/+; R71G10, UAS-Dcr-2/ TRiP.JF03283}attP2 (Dpr18-RNAi)
y, w; UAS-mCD8-GFP/+; R71G10/ TRiP.JF02923 (Dpr20-RNAi)
(D)
y, w; 40A, *Dpr12 Δ ⁵⁰⁻⁸¹*, G13/40A, *Dpr12 Δ ⁵⁰⁻⁸¹*, G13; R71G10, UAS-mCD8-GFP/+
y, w; 40A, *Dpr12 Δ ⁵⁰⁻⁸¹*, G13/40A, *Dpr12 Δ ⁵⁰⁻⁸¹*, G13; R71G10, UAS-mCD8-GFP/+
y, w; 40A, *Dpr12 Δ ⁵⁰⁻⁸¹*, G13/40A, *Dpr12 Δ ⁵⁰⁻⁸¹*, G13; R71G10, UAS-mCD8-GFP/+
y, w; UAS-mCD8-GFP/+; R71G10/+

Figure EV2

- (A) hsFLP, UAS-mCD8-GFP; Gal80, FRT40A/FRT40A; R71G10, UAS-Dcr-2/+
 (B) hsFLP, UAS-mCD8-GFP; Gal80, FRT40A/FRT40A; R71G10, UAS-Dcr-2/
 TRiP.JF03210 (Dpr12-RNAi)
 (D) y, w; UAS-mCD8-GFP/R30G08-p65.AD; R48B03-GAL4.DBD/ +
 (E) y, w; UAS-mCD8-GFP/+; R18H09/ +
 (F) y, w; UAS-mCD8-GFP/+; R48H011/+

Figure EV3

- (C-D) y, w; R71G10-QF2, QUAS-mtdT-HA/+; *DIP-δ^{T2A-Gal4}*/*DIP-δ¹⁻¹¹⁹*
 (E) y, w; R71G10-QF2, QUAS-mtdT-HA/UAS-*DIP-δ*; *DIP-δ^{T2A-Gal4}*/*DIP-δ^{T2A-Gal4}*
 (F) C155-Gal4; UAS-Cas9.P2/+
 (G) C155-Gal4; UAS-Cas9.P2/TKO.GS02451(*gRNA DIP-δ*)
 (H) y, w; R71G10, UAS-mCD8-GFP/ +; UAS-Cas9.C/+
 (I) y, w; R71G10, UAS-mCD8-GFP/ TKO.GS02451(*gRNA DIP-δ*); UAS-Cas9.C/+

Figure EV4

- (A-C) y, w; QUAS-GFP, UAS-mtdT-HA/UAS-tdT; R58E02/R58E02-QF2
 (D-F) y, w; R71G10-QF2, QUAS-mtdT-HA/+; *DIP-δ^{T2A-Gal4}*/+

Figure EV5

- (A) y, w; 40A, *dpr12^{Δ50-81}*, G13/+; R10G03/UAS-mCD8-GFP
 (B) y, w; 40A, *dpr12^{Δ50-81}*, G13/40A, *dpr12^{Δ50-81}*, G13; R10G03/UAS-mCD8-GFP
 (D) y, w; 40A, *dpr12^{Δ50-81}*, G13/+; R48H011/UAS-mCD8-GFP
 (E) y, w; 40A, *dpr12^{Δ50-81}*, G13/40A, *dpr12^{Δ50-81}*, G13; R48H011/UAS-mCD8-GFP
 (G) y, w; 40A, *dpr12^{Δ50-81}*, G13/+; R18H09/UAS-mCD8-GFP
 (H) y, w; 40A, *dpr12^{Δ50-81}*, G13/40A, *dpr12^{Δ50-81}*, G13; R18H09/UAS-mCD8-GFP

Figure EV6

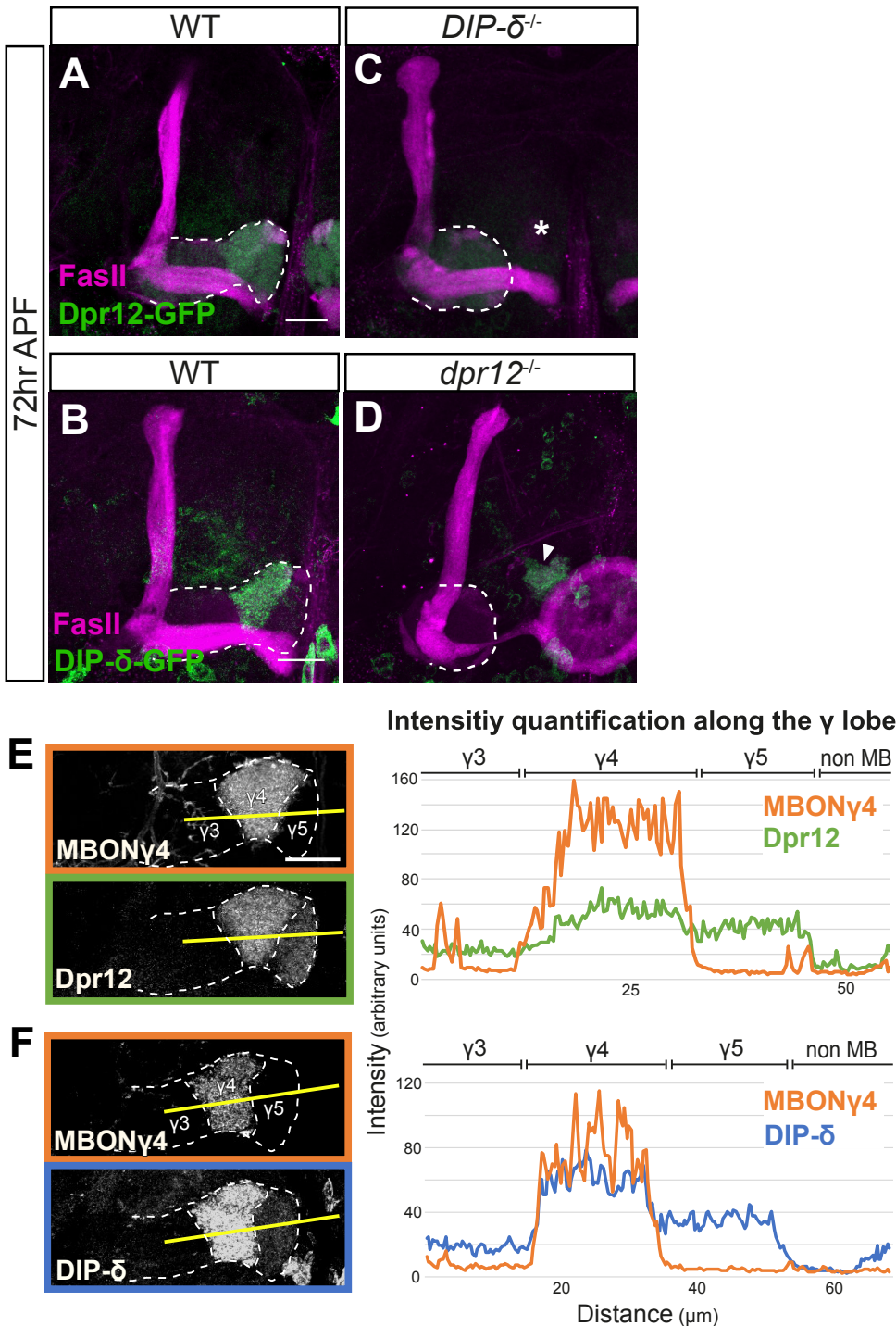
- (A) y, w; R71G10-QF2, QUAS-mtdT-HA/+; *DIP-δ¹⁻¹¹⁹*/*DIP-δ¹⁻¹¹⁹*
 (B) y, w; R71G10-QF2, QUAS-mtdT-HA/+; *DIP-δ¹⁻¹¹⁹*/*DIP-δ¹⁻¹¹⁹*, UAS-DIP-α
 (C) y, w; R71G10-QF2, QUAS-mtdT-HA/+; *DIP-δ^{T2A-Gal4}*/*DIP-δ^{T2A-Gal4}*
 (D) y, w; R71G10-QF2, QUAS-mtdT-HA/UAS-FasII; *DIP-δ^{T2A-Gal4}*/*DIP-δ^{T2A-Gal4}*

Appendix Figure S1

- (A) y, w; Dpr12^{GFSTF}/+
 (B) y, w;; *DIP-δ^{GFSTF}*/+
 (C) y, w; Dpr12^{GFSTF}/+; *DIP-δ^{T2A-Gal4}*/*DIP-δ^{T2A-Gal4}*
 (D) y, w; 40A, *dpr12^{Δ50-81}*, G13/40A, *dpr12^{Δ50-81}*, G13; *DIP-δ^{GFSTF}*/+
 (E) y, w; UAS-CD4-tdT/Dpr12^{GFSTF}; R18H09/+
 (F) y, w; UAS-CD4-tdT/+; *DIP-δ^{GFSTF}*/R18H09

Appendix Figure S2

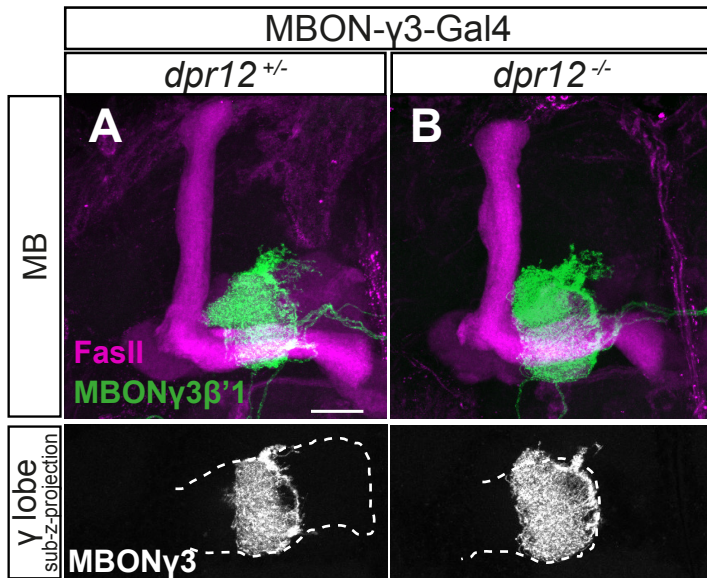
- (A) y,w; 40A, *dpr12^{Δ50-81}*, G13/+; R94B10-GAL4.DBD, R52G04-p65.AD/ UAS-mCD8-GFP
 (B) y,w; 40A, *dpr12^{Δ50-81}*, G13/40A, *dpr12^{Δ50-81}*, G13; R94B10-GAL4.DBD, R52G04-p65.AD/ UAS-mCD8-GFP



Appendix figure S1. Additional data regarding Dpr12 and DIP- δ protein localization, related to Figures 3 and 6.

(A-D) Confocal z-projections of brains expressing either MiMIC mediated Dpr12^{GFSTF} (Dpr12-GFP; A,C) or DIP- δ ^{GFSTF} (DIP- δ -GFP; B,D) fusion proteins, in either WT (A-B), $DIP-\delta^{T2A-Gal4}$ homozygous mutant (C) or $dpr12^{\Delta 50-81}$ homozygous mutant (D) animals at 72hr APF. Green is GFP, magenta is FasII. Dashed line depicts the medial γ -lobe, as determined by FasII staining. Asterisk demarcates the distal part of the lobe; arrowhead demarcates DIP- δ expression at the distal part of the lobe. Scale bar is 20 μ m.

(E-F) Intensity quantification of the indicated channels in the confocal z-projections that appear in Figure 3D (for E) and Figure 3H (for F). Intensity (arbitrary units) was quantified along a defined line that crosses the γ lobe from γ 3 until it exits the MB (marked in yellow; distance is shown in μ m). The MBON- γ 4 channel (GMR18H09-Gal4>CD4-tdT) is shown in orange (E, F), Dpr12-GFP in green (E) and DIP- δ -GFP in blue (F). The rough division to γ -lobe zones is indicated above the graphs. Scale bar is 20 μ m.



Appendix figure S2. MBON-γ3 innervation of the MB γ-lobe in Dpr12 mutant brains, related to Figure 7.

(A-B) Confocal z-projections of *dpr12*^{Δ50-81} heterozygous (A) or homozygous (B) mutant brains expressing membrane-bound GFP (CD8-GFP) driven by MB083C (MBONγ3-Gal4) that is expressed in MBONγ3β'1 (MBON-09). The greyscale channels are sub-z-projections comprised of slices restricted to the γ-lobe (which is outlined in white).

Green and grey are CD8-GFP, magenta is FasII. Scale bar is 20μm.

| Color | Type | Name | Projection Pattern | <i>neuPrint</i> Body ID |
|-------|--------------|--------|---------------------|-------------------------|
| ● | γ-KC | KCym | Medial γ-lobe | 415511327 |
| ● | | KCym | Medial γ-lobe | 415835070 |
| ● | | KCym | Medial γ-lobe | 415835178 |
| ● | | KCym | Medial γ-lobe | 415848228 |
| ● | | KCym | Medial γ-lobe | 415852518 |
| ● | | KCym | Medial γ-lobe | 415908516 |
| ● | | KCym | Medial γ-lobe | 416189410 |
| ● | | KCym | Medial γ-lobe | 416189500 |
| ● | | KCym | Medial γ-lobe | 416598862 |
| ● | | KCym | Medial γ-lobe | 415494049 |
| ● | γ5 PAM-DAN | PAM01 | γ5 compartment | 925799233 |
| ● | | PAM01 | γ5 compartment | 1202397143 |
| ● | | PAM01 | γ5 compartment | 5812982779 |
| ● | | PAM15 | γ5β'2a compartment | 5813096699 |
| ● | γ4 PAM-DAN | PAM08 | γ4 compartment | 580317662 |
| ● | | PAM08 | γ4 compartment | 988852391 |
| ● | γ4>γ1γ2 MBON | MBON05 | γ4>γ1γ2 compartment | 799586652 |
| ● | γ5β'2a MBON | MBON01 | γ5β'2a compartment | 612371421 |

Appendix Table S1. EM-skeletons used for model generation.

A list of the cell types, names, projection patterns, color coding and *neuPrint* IDs for all the EM-based skeletons used to construct the models in Figure 1P and Movie EV1 (see methods for additional details).

| Driver | | Expressing cells | Expression during development | | | Source |
|------------------------|----------------|--|-------------------------------|--|-------|---|
| Name in manuscript | Formal name | | Larva | Pupa | Adult | |
| γ-Gal4 | R71G10-Gal4 | γ-KCs consistently α/β-KCs stochastically | ✓ | ✓ | ✓ | Chr. III: Bl. #39604 Chr. II: Alyagor et al., 2018 |
| γ-QF2 | R71G10-QF2 | γ-KCs consistently α/β-KCs stochastically | ✓ | ✓ | ✓ | This study |
| DIP-δ-Gal4 | DIP-δ-T2A-Gal4 | DIP-δ-expressing cells including PAM-DANs targeting γ4/5 zones | ✓ | ✓ | ✓ | This study |
| PAM-DAN-Gal4 | R58E02-Gal4 | All PAM-DANs | pPAMs* | After 48hr APF | ✓ | BDSC #41347 |
| PAM-DAN-γ3-Gal4 | MB441B | PAM-DANs targeting γ3 | X | ND | ✓ | BDSC #68251 |
| PAM-DAN-γ4-Gal4 | R10G03 | PAM-DANs targeting γ4 | ND | After 72hr APF | ✓ | BDSC #48271 |
| PAM-DAN-γ5-Gal4 | R48H11 | PAM-DANs targeting γ5 | ND | After 72hr APF | ✓ | BDSC #50396 |
| MBON-γ4-Gal4 | R18H09 | MBON-γ4>γ1γ2 (MBON-05) | X | Not at 24hr APF (ND for other time points) | ✓ | BDSC #48830 |
| MBON-γ4-Gal4 | MB298B | MBON-γ4>γ1γ2 (MBON-05) | ND | After 24hr APF | ✓ | BDSC #68309 |
| MBON-γ3-Gal4 | MB083C | MBON-γ3β'1 (MBON-09) | ND | ND | ✓ | BDSC #68287 |
| Pan-Glia-Gal4 | Repo-Gal4 | All glia | ✓ | ✓ | ✓ | BDSC #7415 |
| Pan-KC-Gal4 | OK107-Gal4 | All KCs (γ, α/β and α'/β') | ✓ | ✓ | ✓ | BDSC #854 |
| Pan-Neuron-Gal4 | C155-Gal4 | All neurons | ✓ | ✓ | ✓ | BDSC #458 |

Appendix Table S2. List of drivers used in the current study.

The driver name (in the manuscript and formally), the cells in which it is expressed, and expression throughout development are depicted. ND; not determined. *pPAMs are primary-PAMs which are different from the adult PAM-DANs (data not shown).